Characterisation of the liver progenitor cell niche in liver diseases: potential involvement of Wnt and Notch signalling

Bart Spee, Guido Carpino, Baukje A Schotanus, et al.

Gut 2010 59: 247-257 originally published online November 1, 2009
doi: 10.1136/gut.2009.188367

Characterisation of the liver progenitor cell niche in liver diseases: potential involvement of Wnt and Notch signalling

Bart Spee,[1] Guido Carpino,[2] Baukje A Schotanus,[3] Azeam Katoonizadeh,[1] Sara Vander Borght,[1] Eugenio Gaudio,[4] Tania Roskams[1]

► Supplementary files and a figure are published online only at http://gut.bmj.com/content/vol59/issue2

[1]Department of Morphology and Molecular Pathology, University Hospitals Leuven, Leuven, Belgium [2]Department of Health Sciences, University of Rome 'Foro Italico', Rome, Italy [3]Department of Clinical Sciences of Companion Animals, Faculty of Veterinary Medicine, Utrecht University, The Netherlands [4]Department of Human Anatomy, Sapienza University of Rome, Rome, Italy

Correspondence to
Dr B Spee, Department of Morphology and Molecular Pathology, University Hospitals Leuven, Minderbroederstraat 12, Leuven B3000, Belgium; b.spee@uu.nl

BS and GC contributed equally to this study.

Revised 18 September 2009
Accepted 8 October 2009
Published Online First 1 November 2009

ABSTRACT

Background Hepatic progenitor cells (HPCs) hold a great potential for therapeutic intervention for currently untreatable liver diseases. However, in human diseases molecular mechanisms involved in proliferation and differentiation of HPCs are poorly understood.

Methods and results In the present study activated HPCs and their microenvironment (niche) were investigated in acute and chronic human liver disease by gene-expression analysis and immunohistochemistry/immunofluorescence. Cryopreserved liver tissues were used from patients with parenchymal versus biliary diseases: acute necrotising hepatitis (AH), cirrhosis after hepatitis C infection, and primary biliary cirrhosis in order to study differentiation of HPCs towards hepatocytic versus biliary lineage. Keratin 7 positive HPCs/reactive ductules were captured by means of laser capture microdissection and gene-expression profiles were obtained by using a customised PCR array. Gene expression results were confirmed by immunohistochemistry and immunofluorescence double staining. In all disease groups, microdissected HPCs expressed progenitor cell markers such as *KRT7*, *KRT19*, *NCAM*, *ABCG2*, *LIF*, *KIT*, *OCT4*, *CD44* and *TERT*. In AH, HPCs were most activated and showed a high expression of prominin-1 (CD133) and α-fetoprotein, and a strong activation of the Wnt pathway. In contrast to parenchymal diseases, HPCs in primary biliary cirrhosis (biliary differentiation) showed a high activation of Notch signalling.

Conclusion A distinct pattern of HPC surface markers was found between acute and chronic liver diseases. Similar to what is known from animal experiments, strong evidence has been found signifying the role of Wnt signalling in proliferation of human HPCs whereas Notch signalling is involved in biliary differentiation. These pathways can be targeted in future therapies.

Hepatic progenitor cells (HPCs) are bipotential stem cells that reside in human liver and are able to differentiate towards the hepatocytic or cholangiocytic lineages.[1–4] They can be identified based on their shape as well as by expression of markers such as keratin (K)7, K19 and tumour-associated calcium signal transducer 1 (TACSTD1/EpCAM).[5–7] HPCs are located in the most peripheral branches of the biliary tree (canals of Hering).[8 9] Activated HPCs proliferate and/or differentiate resulting in the formation of reactive ductules (DRs), which are composed of progenitor cells with highly variable marker profiles of which intermediate (transit amplifying) cells of several differentiation states are continuously produced.[10 11]

HPCs are activated in the case of severe cell loss or when the replication of liver parenchymal cells is impaired resulting in proliferation and differentiation towards the cell type which is damaged the most (hepatocytes or cholangiocytes).[12] Furthermore, experimental rat models show that the severity of injury plays an important role in HPC activation; acute hepatocellular damage is able to activate HPCs without differentiation while chronic damage indicates a higher differentiation rate of the progenitor cell compartment.[13] HPC activation and differentiation could be driven by different signals acting onto the niche as result of the stage (acute or chronic) and type of disease (parenchymal or biliary liver disease).[14 15]

The study of other well-described stem cell niches in other organs (intestinal, hair-follicle and haematopoietic stem cell compartment) has indicated that Wnt and Notch signalling pathways are important for the regulation of stem-cell proliferation and differentiation towards committed lineages.[16–19] Wnt and Notch signalling pathways have been shown to play a key role during embryonic liver development.[20–27] In addition, studies on toxin-induced murine models suggest a role of these pathways in adult liver.[28–31]

The aim of this study was to investigate HPC surface markers and proliferation/differentiation signals from its niche in parenchymal and biliary liver diseases. To achieve this, gene-expression profiles were generated from microdissected K7-positive cells in different liver diseases; acute hepatitis (AH), post-hepatitis C virus (HCV) liver cirrhosis, and primary biliary cirrhosis (PBC). Immunohistochemistry (IHC) and immunofluorescence were used to confirm the gene-expression profile obtained. The results provide insight into the role of Wnt and Notch signalling in proliferation and differentiation of HPCs during parenchymal and biliary liver diseases in humans.

MATERIALS AND METHODS

Liver specimens

All human liver specimens consisted of rest material of liver explants taken for diagnostic/therapeutic purposes. The liver explants were diagnosed for acute hepatitis with submassive liver cell necrosis (AH), post-HCV liver cirrhosis (HCV), and PBC in Ludwig stage IV. The aetiology for the AH group included acute hepatitis B infection as well as drug-induced AH. Resection specimens from

normal-appearing liver with no histological abnormalities were derived from liver sections surrounding focal nodular hyperplasia or colon metastasis and used as control samples (H). For routine diagnosis samples were fixed in 6% formalin or in B5 fixative and embedded in paraffin. For microdissection and RNA isolation, samples were embedded in OCT compound (Miles, Kankakee, Illinois, USA), snap-frozen in liquid nitrogen cooled isopentane and stored at −80°C until further use. For assessment of histopathology and fibrosis, the sections were stained with haematoxylin–eosin, PAS diastase, Hall's bilirubin and Sirius red.

Keratin 7 antibody-guided laser capture microdissection

All buffers and solutions were prepared with diethylenepyrocarbonate (DEPC)-treated water (Ambion, Austin, Texas, USA). All used glassware was treated with RNase Zap (Ambion) and washed three times with DEPC-treated water prior to use. Antibody incubations and DAB procedures were performed in the presence of 0.4 U/μl SUPERase RNase Inhibitor (Ambion). Thick frozen sections (10 μm) of human liver (n=4 per group) were cut using RNase-free blades, mounted on precooled (4°C) RNase-free PEN membrane slides (P.A.L.M.; MicroLaser Technologies, Bernried, Germany), immediately placed on dry ice, and stored for up to 1 week at −80°C. Rapid immunohistochemical staining was performed on one slide at a time, to optimise speed of handling. Before laser capture microdissection (LCM), frozen sections were taken from −80°C storage, immediately fixed in ice-cold acetone (−20°C for 5 min) and washed briefly (3–5 s) in phosphate-buffered saline (PBS). Sections were incubated with anti-human K7 (1:20 in PBS for 7 min at room temperature (RT); Dako, Glostrum, Denmark; M7018), briefly washed in PBS, and subsequently incubated with EnVision goat anti-mouse peroxidase-conjugated antibody (undiluted for 7 min at RT; Dako; K4006). The signal was developed with DAB solution (0.06% 3,3′-diaminobenzidine in PBS, 0.003% H_2O_2) for 3 min. Sections were dehydrated in an ethanol series (75–95–100%, 15 s each). The LCM procedure was performed on the P.A.L.M. Microbeam II with an Axiovert-200 microscope (P.A.L.M.). Keratin 7 reactive ductules were dissected (for examples see supplementary file 1), avoiding cholestatic hepatocytes (in PBC) and differentiating intermediate hepatocytes in AH and HCV (for examples see supplementary file 2). The laser-dissected cells were then ejected from the slide with a single defocused laser pulse and catapulted directly into an adhesive cap (P.A.L.M.). Cells were collected within 25 min. Afterwards, 50 μl of lysis buffer (Ambion) was added to the adhesive cap and vortexed upside down. Lysates were collected by centrifugation (14 000 *g*, 5 min), snap frozen in liquid nitrogen and stored at −80°C until further use.

RNA isolation and amplification

From each liver sample, four LCM samples were pooled for total RNA extraction using the RNAqueous-Micro kit (Ambion). The RNA isolation included an additional DNase treatment (0.1 U/μl) to exclude DNA contamination (Ambion). RNA quality after LCM was determined with an Agilent BioAnalyzer-2100 (Agilent, Palo Alto, California, USA) in combination with RNA 6000 Pico-LabChip. The RNA was amplified with the WT-Ovation Pico RNA Amplification System (NuGEN Technologies, Bemmel, The Netherlands). The WT-Ovation RNA amplification system reverse transcribes RNA to cDNA, which is amplified during the so-called SPIA amplification, a linear isothermal DNA amplification process,[32] resulting in end-products of single-strand DNA (ssDNA). The amplified product was purified with DNA Clean&Concentrator-25 kits from Zymo research (Baseclear Lab Products, Leiden, The Netherlands). The amplified products were diluted three times and stored at −20°C until use.

Gene-expression measurements

All qPCR experiments were conducted with a MyiQ Single-Colour Real-Time PCR Detection System (BioRad, Veenendaal, the Netherlands). For PCR array experiments, a RT2 Profiler Custom PCR Array was used to simultaneously examine the mRNA levels of the genes of interest and five reference genes (see supplementary file 3), according to the protocol of the manufacturer (SuperArray Bioscience, Frederick, Maryland, USA). A total volume of 25 μl of PCR mixture, which included 12.5 μl of RT2 Real-Time SYBR Green/Fluorescein PCR master mix from SuperArray Bioscience, 11.5 μl of milliQ, and 1 μl of template cDNA, was loaded in each well of the PCR array. PCR amplification was conducted with an initial 10-min step at 95°C followed by 40 cycles of 95°C for 15 s and 60°C for 1 min. Data were analysed using the comparative cycle threshold method with normalisation of the raw data to reference genes including 18S ribosomal RNA (18SrRNA), hypoxanthine phosphoribosyltransferase 1 (HPRT), ribosomal protein L13a (RPL13A), glyceraldehyde-3-phosphate dehydrogenase (GAPDH), and β-actin (ACTB).

Statistical analysis of gene expression measurements

For gene-expression measurements, the relative gene expression of each gene-product was used as the basis for all comparisons. The results were assessed for normality using the Kolmogorov–Smirnoff and the Levene tests. The data were not normally distributed; therefore the non-parametric (Kruskal–Wallis) analysis of variance was used for all comparisons. Post-test analysis was performed with a Mann–Whitney U test. Analysis was performed using SPSS software (SPSS Benelux, Gorinchem, The Netherlands). A p value less than 0.05 was considered statistically significant.

Immunohistochemistry

IHC was performed both on serially cut cryostat sections (5 μm) and on serially cut paraffin embedded sections (4 μm). For IHC on snap frozen samples (H (n=5), AH (n=10), HCV (n=10), and PBC (n=10)), sections were fixed in acetone for 10 min. Endogenous peroxidase activity was blocked in Dual Endogenous-Enzyme Blocking Reagent (Dako) for 10 min at RT. Afterwards, sections were rinsed in PBS (pH 7.4) and incubated with primary antibody for 1 h at RT (table 1). Samples were rinsed with PBS for 5 min, then incubated for 30 min at room temperature with EnVision (Dako), developed with AEC (Dako) and counterstained with Mayer's haematoxylin. For IHC on paraffin sections (H (n=5), AH (n=10), HCV (n=10), and PBC (n=10)), endogenous peroxidase activity was blocked in methanolic hydrogen peroxide (2.5%) for 30 min at RT. Antigen retrieval was performed as described in table 1. For heat-induced antigen retrieval sections were incubated in citrate buffer (Dako S2031) for 30 min in a water bath at 96°C and cooled down 10 min at RT. Sections were rinsed in PBS (pH 7.4) and incubated with primary antibody for 1 h at RT or at 4°C overnight (table 1). Samples were rinsed with PBS for 5 min, and incubated for 30 min at room temperature with EnVision (Dako). The signal was developed in DAB solution (0.06% 3,3′-diaminobenzidine in PBS, 0.003% H_2O_2) for 5 min and counterstained with Mayer's haematoxylin. Negative controls included omission of the primary antibody.

Statistical analysis of immunohistochemistry

Evaluation of IHC was performed by calculating the average number of IHC-positive HPCs per field using a 20 times objective

Table 1 Immunohistochemical/immunofluorescence reagents and methods

Antibody	Type	Antigen retrieval	Dilution	Incubation	Code	Manufacturer
Anti-keratin 7	Mouse monoclonal	Heat-induced	1:50	1 h RT	M7018	Dako
Anti-CD133	Mouse monoclonal	Heat-induced	1:50	4°C o/n (par) 1 h RT (fr)	ab5558	Abcam, Cambridge, UK
Anti-NCAM1	Mouse monoclonal	Heat-induced	1:50	1 h RT	CD56-1B6	Novacastra, Zaventem, Belgium
Anti-β-catenin	Mouse monoclonal	Heat-induced	1:50	1 h RT	M3539	Dako
Anti-Jagged-1	Mouse monoclonal	Frozen sections only	1:50	1 h RT	Sc-6011	Santa Cruz, Heidelberg, Germany
Anti-LEF1	Mouse monoclonal	No antigen retrieval	1:50	1 h RT	ab22884	Abcam
Anti-Notch1/NICD (IF)	Rabbit polyclonal	Frozen sections only	1:100	4°C o/n	Sc-6014	Santa Cruz
Anti-β-catenin (IF)	Rabbit polyclonal	Frozen sections only	1:50	4°C o/n	ab2982	Abcam

Fr, frozen sections; IF, immunofluorescence; Par, paraffin sections.

counted in three to five non-overlapping fields. IHC determination was performed independently and blindly by two independent investigators (TR and GC). Data were expressed as mean ± standard deviation (SD). Statistics were performed using the Mann–Whitney U test and Spearman's correlation coefficient. A p value less than 0.05 was considered statistically significant.

Immunofluorescence

In order to confirm the gene-expression profiling of Wnt and Notch activation, downstream nuclear transcription factors (β-catenin and Notch-1 intracellular domain (Notch1/NICD) were examined. Immunofluorescence double staining was performed to identify (nuclear) staining in K7 positive cells on 10 μm cryosections, with parallel antibody incubations directed against K7 and β-catenin, or K7 and Notch1/NICD. The nuclei were stained with ToPro3. Slides (AH (n=4), HCV (n=4), and PBC (n=4)) were incubated with mixed primary antibodies overnight at 4°C (table 1), and with mixed secondary antibodies, Alexa 488 goat anti-mouse and Alexa 568 goat anti-rabbit (Invitrogen, Breda, The Netherlands), at RT for 30 min. Counterstain was performed with ToPro-3 (Invitrogen) for 20 min. Rinsing steps were performed in TBS with 0.1% Tween 20, and slides were covered with Aquamount (Vector Laboratories, Burlingame, California, USA). Pictures were obtained by a Leica TCS SP confocal microscope (Leica microsystems, Rijswijk, the Netherlands) with an argon laser at 488 nm, a krypton laser at 568 nm, and a helium/neon laser at 633 nm.

RESULTS

Gene-expression profiling

Gene expression profiles (figures 1–3) were determined from microdissected (activated) liver progenitor cells/ductular reaction (HPCs/DR) from several liver diseases; AH, (n=4), HCV (n=4), and PBC (n=4). Examples of microdissected HPCs/DR see supplementary figure 1. RNA quality measurements (RIN value from 0 to 10) indicated good quality RNA starting material (range 6.8–8.4), and medium quality RNA after microdissection (range 4.0–6.9). Expression of stem cell markers including prominin 1 (*CD133*), α-fetoprotein (*AFP*), neural cell adhesion molecule (*NCAM*), keratin 19 (*KRT19*), keratin 7 (*KRT7*), ATP-binding cassette, subfamily G, member 2 (*ABCG2/BCRP*), leukaemia inhibitory factor V-KIT Hardy–Zuckerman 4 feline sarcoma viral oncogene homolog (*KIT/SCFR*), Pou domain, class 5, transcription factor 1 (*OCT4/POU5F1*), CD44 antigen (*CD44*), oestrogen-related receptor β (*ESRRB*), homeobox transcription factor NANOG (*NANOG*), and telomerase reverse transcriptase (*TERT*), were all present in microdissected HPCs/DR (figure 1). *CD133* and *AFP* were more prominently expressed in AH versus HCV and PBC. *NCAM* was highly expressed in AH and PBC but lower in HCV. Both *KRT19, KRT7* and *LIF* were highly expressed in HCV although not statistically different towards PBC. *OCT4* was more prominently expressed in HCV versus AH and PBC. *ABCG2*, *KIT*, *CD44,* and *TERT* were similarly expressed in the disease groups. From the 'stemness' genes, gene expression of *ESRRB* and *NANOG* was induced in PBC compared to AH and HCV. The most prominent expressed mesenchymal marker in all three groups was glial fibrillary acidic protein (*GFAP*), while desmin (*DES*), a marker of myofibroblasts, was more prominently expressed in PBC.

From the Wnt signalling pathway (figure 2), the ligands wingless-type MMTV integration site family (*WNT)3A* and *WNT5* were most prominently expressed in AH, HCV and PBC. Wnt receptor frizzled 1 (*FZD1*) was more prominently expressed in HCV although not statistically different towards PBC. *WNT1*, *WNT4* and axis inhibitor 2 (*AXIN2*) were all equally expressed in AH, HCV and PBC. Glycogen synthase kinase 3-β (*GSK3B*) expression was elevated in HCV although not statistically different form AH. The lowest expression of adenomatous polyposis coli (*APC*) (necessary for downregulation of β-catenin) was found in AH while it increased significantly in HCV and was highly expressed in PBC. Lymphoid enhancer-binding factor 1 (*LEF1*), a transcription factor from the T cell-specific transcription factor/lymphoid enhancer factor-1 (TCF/LEF1) family, which is activated by intracellular protein β-catenin, was significantly expressed in all diseases with the highest expression in PBC.

From the Notch signalling pathway (figure 3) δ-like (*DLL*) 1 was highly expressed in AH whereas Jagged-1 (*JAG1*), from the serrate ligands, was upregulated in PBC. *DLL3*, *DLL4* and Jagged-2 (*JAG2*) were equally expressed in AH, HCV and PBC. Notch, drosophila, homolog of (*NOTCH*) 1 expression was highest in HCV, while *NOTCH4* expression in HCV was lower than PBC. No differences in *NOTCH2* and *NOTCH3* expression was found in AH, HCV and PBC. The most prominent receptors were *NOTCH1* and *NOTCH3*.

Immunohistochemistry

To confirm gene-expression profiles and to compare to histologically healthy liver samples, IHC for K7, NCAM, prominin-1 (CD133), β-catenin, LEF1 (transcription factor of an active Wnt signalling pathway), and Jagged-1 (JAG1) was performed on a larger (n=30) series of patients. Examples of immunohistochemical findings are provided in figure 4. The average amounts of positive HPCs per microscopic field are provided in tables 2 and 3.

In histologically healthy liver, small amounts of K7 positive cells are seen in the periportal region (10.2±1.3, figure 4A). Compared to healthy livers, the number of K7 positive cells is diffusely increased in AH (72.9±8.2, figure 4B) and HCV

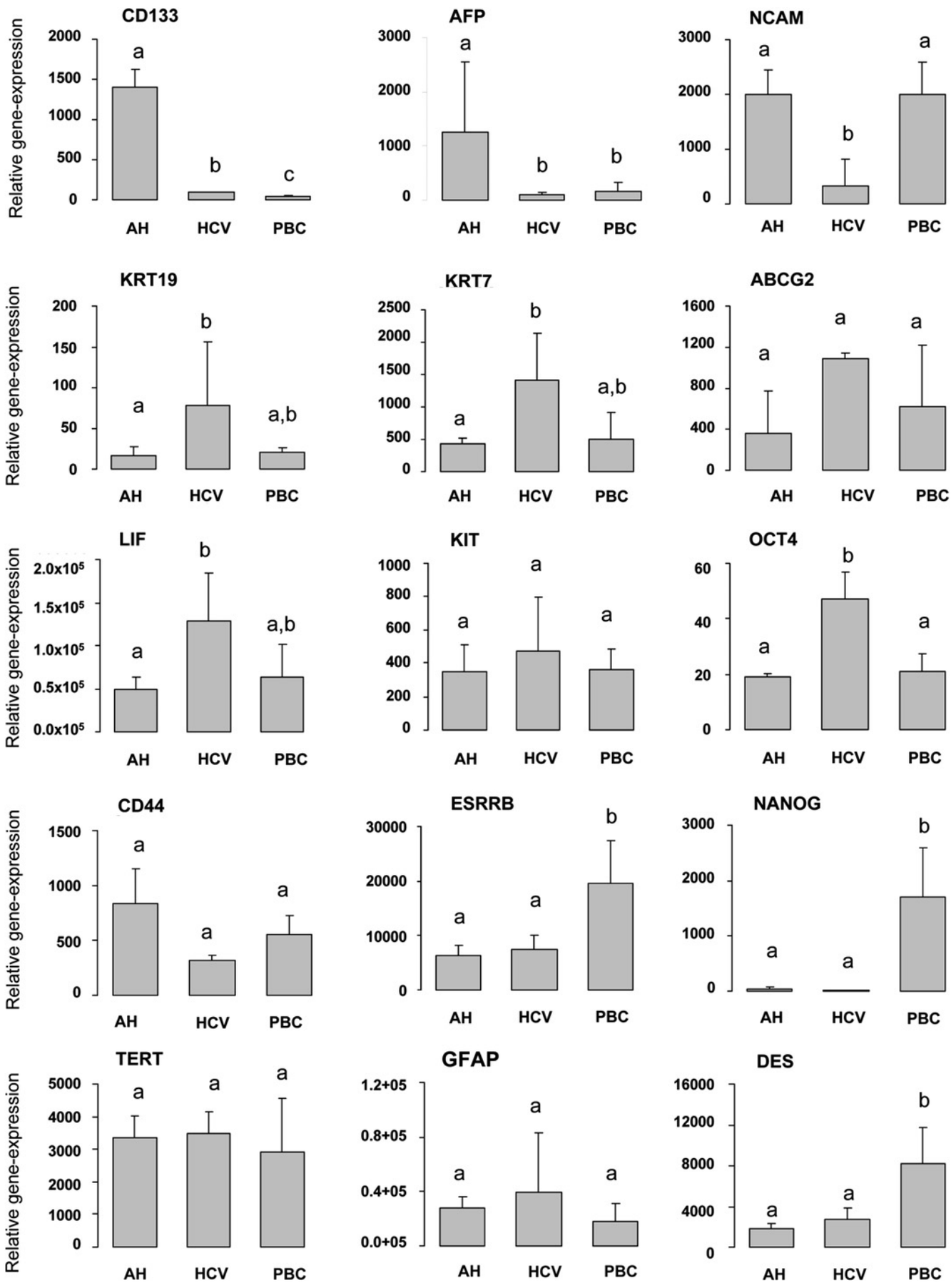

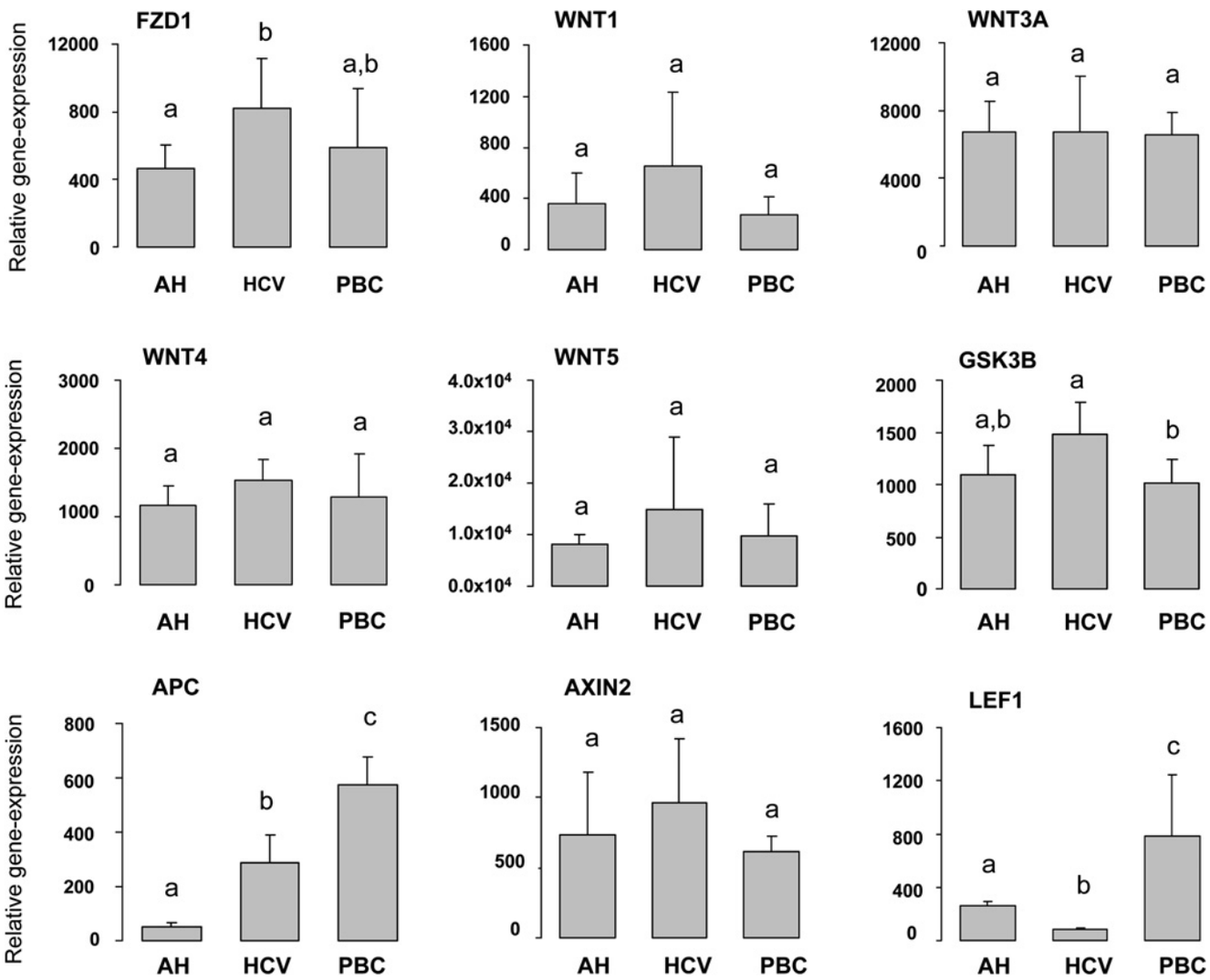

Figure 2 Gene-expression profile of Wnt signalling pathway. Bar graphs indicate relative expression of mRNA levels in acute hepatitis with submassive liver cell necrosis (AH, n=4), post-hepatitis C virus liver cirrhosis (HCV, n=4), and primary biliary cirrhosis in Ludwig stage IV (PBC, n=4). Different letters above bars indicate statistical significance ($p<0.05$). APC, adenomatous polyposis coli; AXIN2, axis inhibitor 2; FZD1, frizzled 1; GSK3B, glycogen synthase kinase 3-beta; LEF1, lymphoid enhancer-binding factor 1; WNT, wingless-type MMTV integration site family.

(41.3±5.8, figure 4C), and is increased in the fibrous septa and (septal) interface in PBC (45.3±6.1, figure 4D). In histologically healthy liver, scarce numbers of CD133 positive HPCs with an apical staining pattern are located in the canals of Hering (1.2±0.5, figure 4E). Besides these HPCs and some occasional CD133 positive cholangiocytes, no other cell types were positive. In AH, the highest amount of CD133 positive HPCs is found in a diffuse pattern (34.0±7.0, figure 4F). CD133 positive HPCs are mainly located into the fibrous septa in HCV (7.3±1.8, figure 4G) and PBC (5.9±1.9 figure 4H). In histologically healthy liver, numerous NCAM-positive lobular hepatic stellate cells and NCAM-positive nerves and nerve endings are seen, while positive NCAM staining of interlobular bile ducts is rare. Some NCAM-positive HPCs were found periportally (2.3±1.1, figure 4I). A high number of NCAM-positive HPCs were diffusely found in AH (64.4±8.9, figure 4J). NCAM-positive HPCs were located in the fibrous septa and interface in HCV (18.1±4.2, figure 4K) and PBC (30.9±5.3, figure 4L). In histologically healthy liver, rare JAG1-positive HPCs, some JAG1-positive bile ducts and no JAG1-positive hepatocytes or endothelial cells are seen (figure 4M). Numerous JAG1-positive HPCs are present in AH (35.6±8.6, figure 4N), HCV (16.6±9.5, figure 4O) and PBC (31.6±6.1, figure 4P). In histologically healthy liver, β-catenin is mostly expressed on the cell membrane of HPCs, cholangiocytes and hepatocytes (figure 4Q). In contrast, β-catenin is expressed in the cytoplasm and nuclei in HPCs in AH (22.0±7.6, figure 4R),

Figure 1 **[See page 250]** Gene-expression profile of stem-cell markers. Bar graphs indicate relative expression of mRNA levels in acute hepatitis with submassive liver cell necrosis (AH, n=4), post-HCV liver cirrhosis (HCV, n=4), and primary biliary cirrhosis in Ludwig stage IV (PBC, n=4). Different letters above bars indicate statistical significance ($p<0.05$). ABCG, ATP-binding cassette, subfamily G, member 2 (BCRP); AFP, α-fetoprotein; DES, desmin; ESRRB, oestrogen-related receptor beta; GFAP, glial fibrillary acidic protein; KRT, keratin; LIF, leukaemia inhibitory factor; KIT, V-KIT Hardy–Zuckerman 4 feline sarcoma viral oncogene homologue (SCFR); NANOG, homeobox transcription factor NANOG; NCAM, neural cell adhesion molecule; OCT, Pou domain, class 5, transcription factor 1 (POU5F1); TERT, telomerase reverse transcriptase.

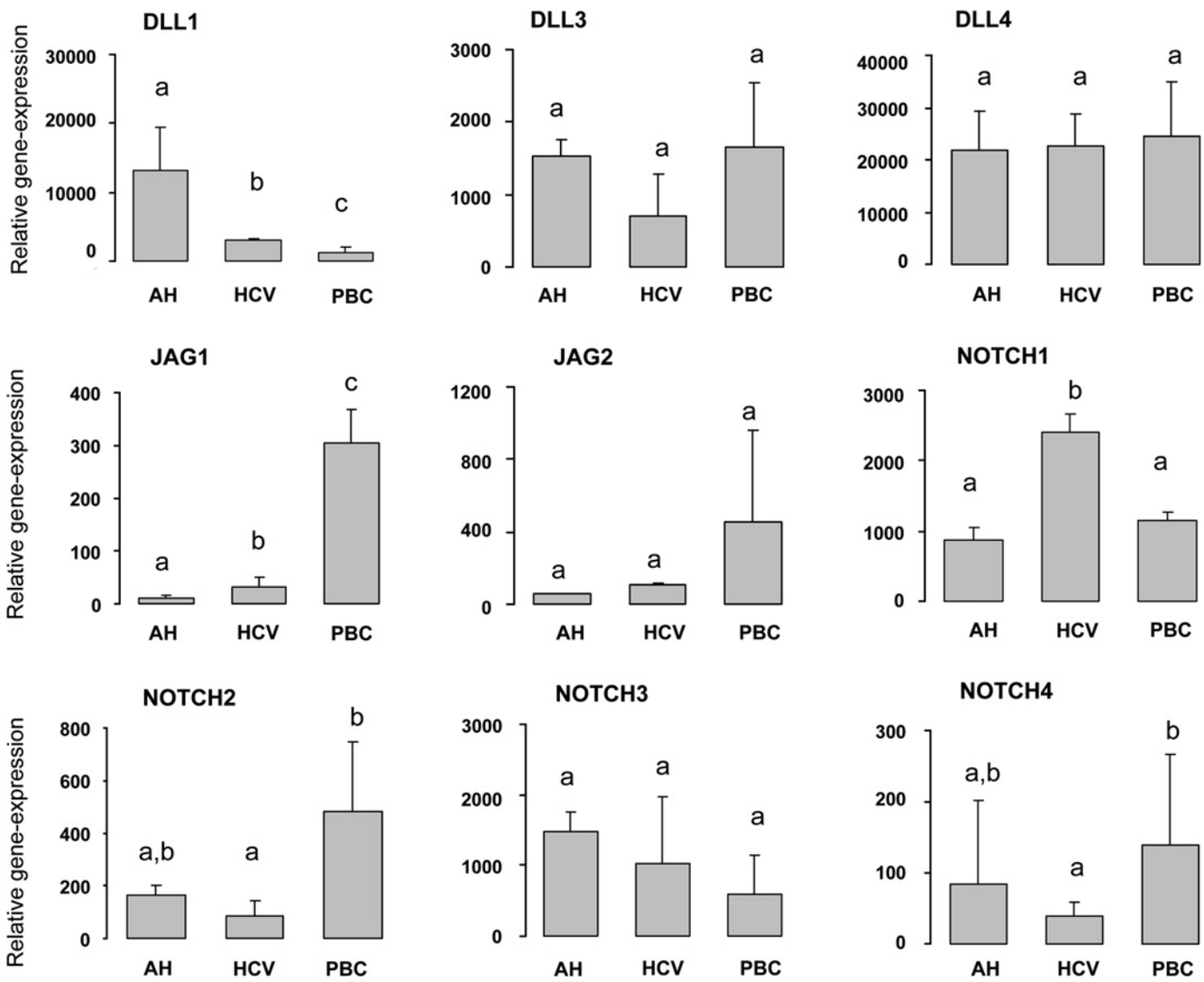

Figure 3 Gene-expression profile of the Notch signalling pathway. Bar graphs indicate relative expression of mRNA levels in acute hepatitis with submassive liver cell necrosis (AH, n=4), post-hepatitis C virus liver cirrhosis (HCV, n=4), and primary biliary cirrhosis in Ludwig stage IV (PBC, n=4). Different letters above bars indicate statistical significance ($p<0.05$). DLL, delta-like; JAG, Jagged; NOTCH, Notch, *Drosophila*, homologue of;

HCV (9.6±3.6, figure 4S), and PBC (20.2±7.3, figure 4T). In histologically healthy liver, a moderate diffuse staining of LEF1 in hepatocytes was observed (figure 4U). LEF1 is highly positive in the nuclei of HPCs in AH (35.2±7.1, figure 4V) and in PBC (41.0±11.0, figure 4X), while a lower expression is found in HCV (13.0±4.7, figure 4W).

Immunofluorescence

To confirm a possible activation of Wnt and Notch pathways in HPCs/DR, immunofluorescence double staining was performed by using antibodies directed against K7 and β-catenin (figure 5A) or K7 and Notch1/NICD (figure 5B). In all diseases, the most prominent β-catenin staining was found on parenchymal cells and confirmed the immunohistochemical staining. Double staining of K7 and β-catenin was largely found in AH and to a lesser extent in HCV and PBC. The nuclear presence of β-catenin was mostly in AH (figure 5A). In all diseases, Notch1/NICD staining showed a diffuse cytoplasmic staining of hepatocytes. Some of the bile ducts and some portal fibroblasts stained positive (cytoplasmic). Other portal structures and the central vein were negative. Double staining of K7 and Notch/NICD as well as nuclear localisation of Notch/NICD in HPCs was predominantly found in PBC, whereas little to no nuclear staining of HPCs was found in HCV or AH (figure 5B).

DISCUSSION

HPCs represent a reserve cell compartment that is activated when the mature epithelial cells of the liver (hepatocytes and cholangiocytes) are damaged or inhibited in their replication.[33] In the human liver, HPCs are activated after acute and chronic damage.[34] Different subpopulations of HPCs could be described considering their phenotype and their differentiation depending on the type and severity of the disease.[35] In the present study, we have used microdissection and gene-expression profiling to study the proliferation and differentiation of HPCs in three different liver diseases: an acute disease with prevalent hepatocellular damage (AH), chronic hepatocellular disease (HCV) and primary biliary disease (PBC). Results of this study led to the proposed model of HPC activation and differentiation as summarised in figure 6.

HPCs represent a dynamic cellular compartment and the severity and duration of injury play an important role in HPC proliferation and differentiation. The expression of CD133 is

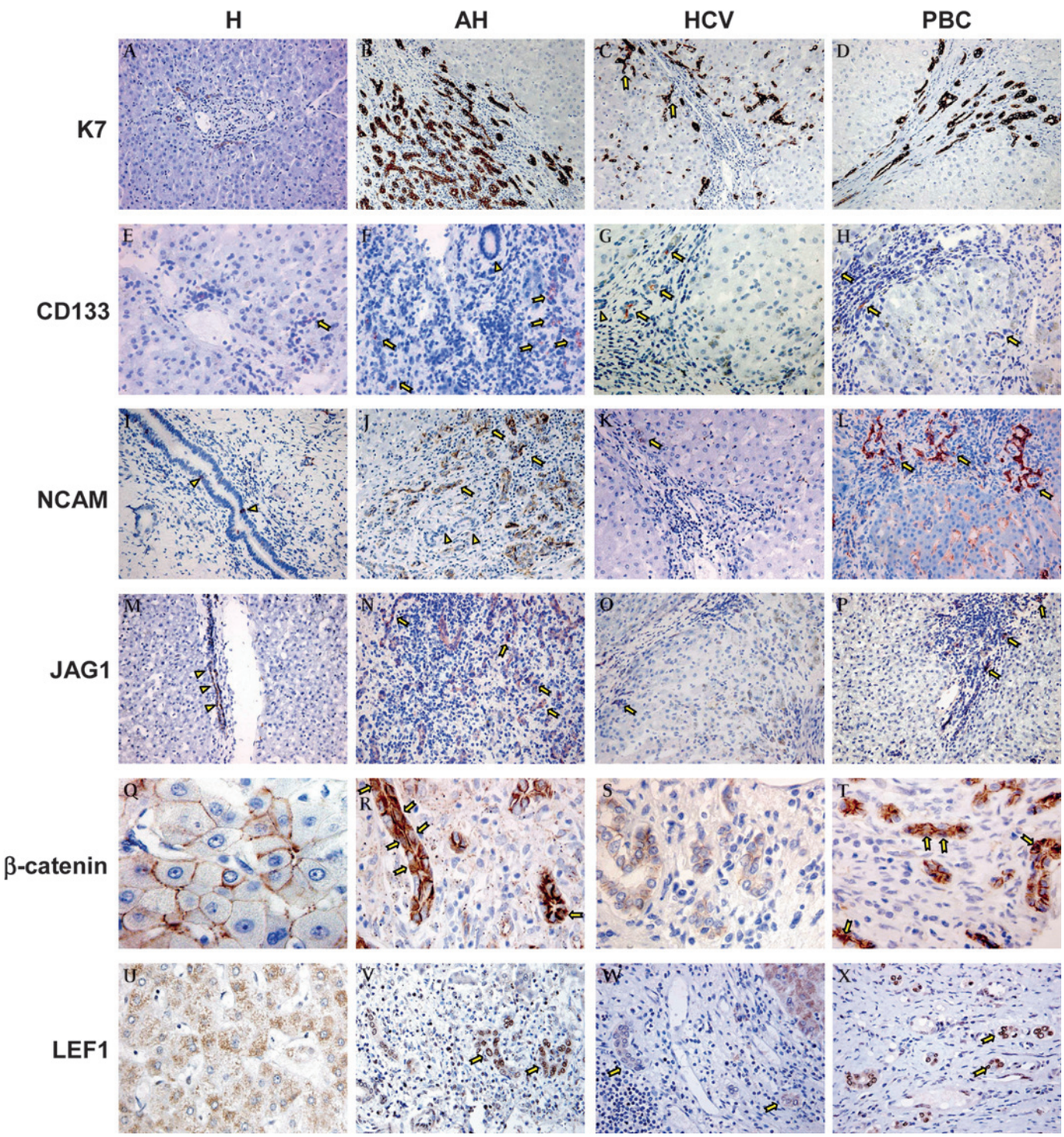

Figure 4 Immunohistochemical staining. Examples of K7 (A—D), CD133 (E—H), NCAM (I—L), JAG1 (M—Q), β-catenin (P—T) and LEF1 (U—X) stainings in histologically healthy livers (H), acute hepatitis with submassive liver cell necrosis (AH, n=4), post-hepatitis C virus liver cirrhosis (HCV, n=4), and primary biliary cirrhosis in Ludwig stage IV (PBC, n=4). Original magnification: ×20 (A—P, U—X) or ×40 (Q—T). Arrows indicate progenitor cells and arrowheads interlobular bile ducts. CD133, prominin 1; JAG1, Jagged-1; K7, keratin 7; LEF1, lymphoid enhancer-binding factor 1; NCAM, neural cell adhesion molecule.

usually found in uncommitted progenitor cells.[36] In addition, CD133 correlates with AFP, which has been previously confirmed in hepatocellular carcinomas with CD133 expression.[37] In AH, HPCs proliferate in large numbers and diffusely express NCAM, AFP and CD133 suggesting that these HPCs represent a subtype of HPCs during this acute activation after submassive hepatocyte necrosis. In contrast, HPC activation in HCV is less pronounced as indicated by the decreased number of K7-positive HPCs (table 2). In HCV few CD133-positive HPCs were found suggesting a more differentiated (committed towards hepatocytic lineage) state of these cells during this chronic lower degree of hepatocyte damage. In PBC, the HPC compartment has a prominent activation as indicated by the number of K7-positive HPCs. HPCs in PBC have a pronounced NCAM expression; however, fewer

Table 2 Immunohistochemical characterisation with progenitor cell markers: the number of immunohistochemically positive hepatic progenitor cells (HPCs) in normal liver (H), acute hepatitis with submassive necrosis (AH), hepatitis C-related cirrhosis (HCV) and primary biliary cirrhosis (PBC)

	K7	CD133	NCAM
H	10.2±1.3* (periportal)	1.2±0.5* (periportal)	2.3±1.1* (periportal)
AH	72.9±8.2† (diffuse)	34.0±7.0† (diffuse)	64.4±8.9† (diffuse)
HCV	41.3±5.8 (diffuse)	7.3±1.8 (fibrous septa)	18.1±4.2 (fibrous septa/interface)
PBC	45.3±6.1 (fibrous septa/interface)	5.9±1.9 (fibrous septa)	30.9±5.3‡ (fibrous septa/interface)

Data are expressed as mean ± standard deviation. The most prominent location of the positively stained HPCs is provided between the brackets.
Spearman correlation:
*$p<0.001$ vs AH, HCV, and PBC; †$p<0.001$ vs HCV, and PBC; ‡$p<0.001$ vs HCV.
CD133, prominin; K7, keratin 7; NCAM, neural cell adhesion molecule.

Table 3 Immunohistochemical characterisation of Wnt effectors and Notch ligand: the number of immunohistochemically positive hepatic progenitor cells (HPCs) in acute hepatitis with submassive necrosis (AH), hepatitis C-related cirrhosis (HCV) and primary biliary cirrhosis (PBC)

	JAG1	β-Catenin	LEF1
AH	35.6±8.6	22.0±7.6	35.2±7.1
HCV	16.6±9.5*	9.6±3.6*	13.0±4.7†
PBC	31.6±6.1	20.2±7.3	41.0±11.0

Data are expressed as mean ± standard deviation.
*$p<0.02$ versus AH and PBC; †$p<0.001$ versus AH and PBC.
JAG1, Jagged-1; LEF1, lymphoid enhancer-binding factor 1.

CD133-positive HPCs are present indicating that the HPCs are in a more differentiated state (committed towards biliary lineage) compared to AH.[38] CD133-positive cells may therefore identify a more restricted population of progenitor cells, which are maximally activated after submassive acute necrosis of hepatocytes. The presence of CD133-positive cells raises the question of whether these cells derive from haematopoietic stem cells or represent the resident HPC compartment.[12 39] CD133-positive HPCs have been detected in conditions (eg, healthy liver) in which a bone marrow contribution is absent or minimal suggesting that these cells should represent resident HPCs.[40 41] Recently, CD133-positive hepatic stellate cells have been described as progenitor cells in rats.[42] Although the possibility of a mesenchymal cell type with CD133 positivity cannot be excluded, the cells in healthy liver appear epithelial in nature. Taken together, CD133 is a marker for activated progenitors in acute phases of hepatocytic liver disease and is correlated with an increased AFP expression.

In AH, activated HPCs predominantly proliferate rather than differentiate.[17 43] HPC activation plays a key role in the prognosis of this pathology as indicated previously.[44] Although HPCs massively proliferate in AH, the differentiation towards hepatocytes takes place only after 1 week from the initial liver injury. This delay in differentiation in turn affects the outcome of the patients with AH. The Wnt pathway, which has a key role in stimulating stem cell proliferation,[45] is more pronounced in AH compared to HCV or PBC (figures 2, 4 and 5). The important role of the Wnt pathway in HPC activation/proliferation was described before in several in vitro assays as well as in murine HPC proliferation models.[28 30 46 47] The similar activation of Wnt in AH compared to these toxin-induced murine models underlines the importance of this pathway in human liver diseases with an acute onset.

Terminal differentiation of HPCs is characterised by the loss of NCAM.[48] In PBC the majority of HPCs are NCAM positive indicating their decreased capacity for terminal differentiation into mature cholangiocytes (characterised by the loss of NCAM expression), although some NCAM negative HPCs remain. As

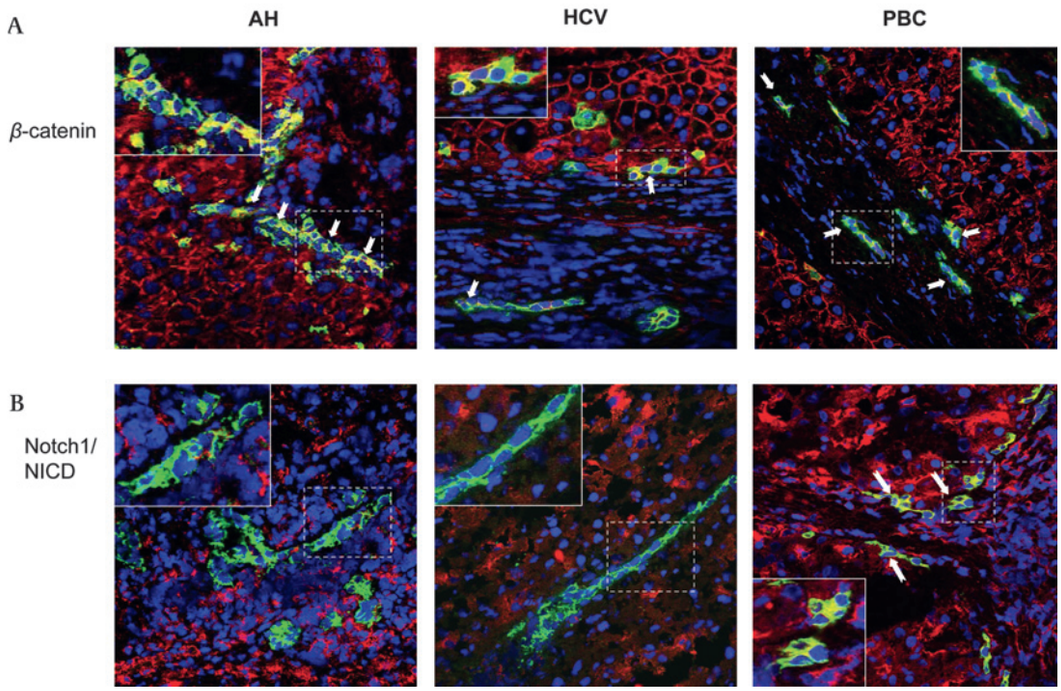

Figure 5 Immunofluorescence staining. Examples of immunofluorescence double staining with (A) β-catenin (red) and K7 (green) and (B) Notch1 intracellular domain (NICD, red) and K7 (green) in acute hepatitis with submassive liver cell necrosis (AH, n=4), post-hepatitis C virus liver cirrhosis (HCV, n=4), and primary biliary cirrhosis in Ludwig stage IV (PBC, n=4). Counter stain Topro-3 (blue). Original magnification: 4×40 (insets ×80). Arrows indicate examples of nuclear staining in K7 positive cells.

A

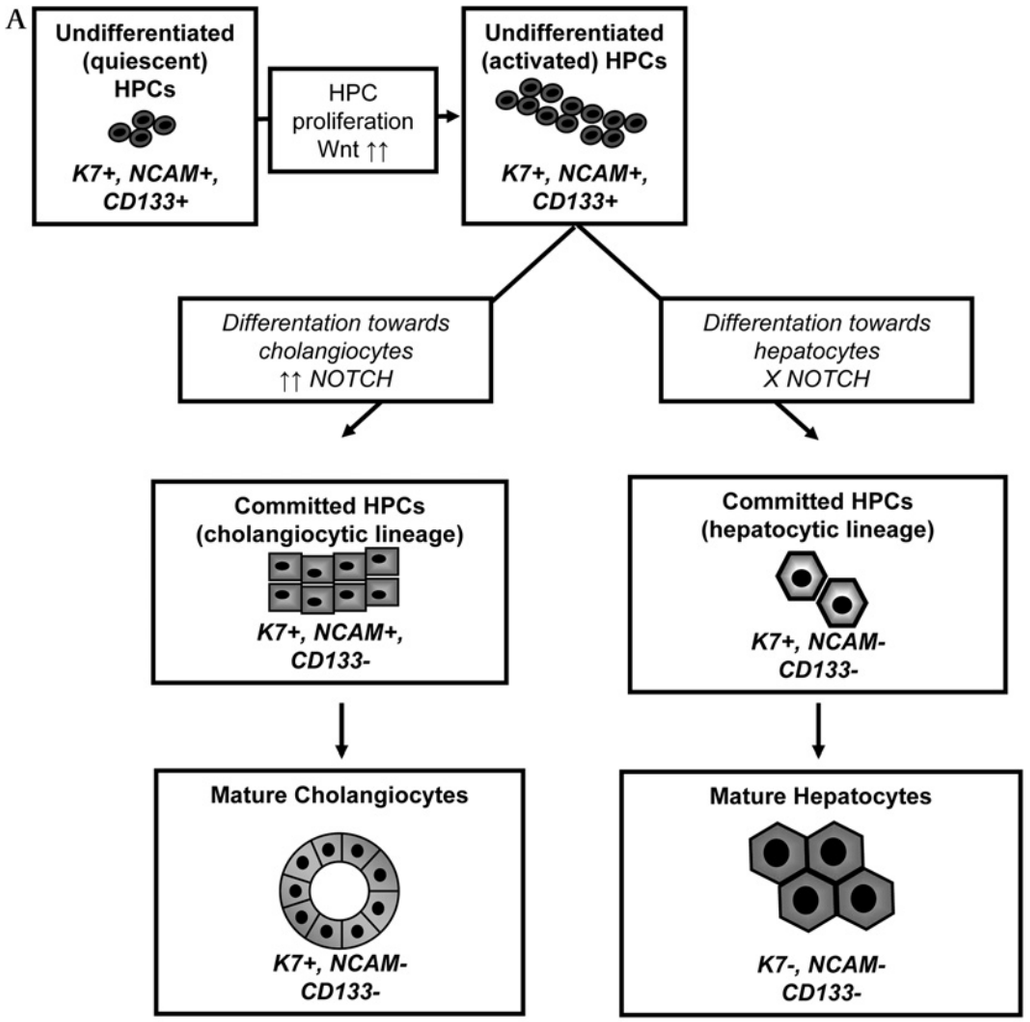

B

	Acute Hepatocytic Damage (AH)	Chronic Hepatocytic Damage (HCV)	Chronic Cholangiocytic Damage (PBC)
K7	↑↑↑	↑↑↑	↑↑↑
NCAM	↑↑↑	x	↑↑↑
CD133	↑↑↑	↑	↑
Predominant HPC subpopulation	CK7+/NCAM+/CD133+	CK7+/NCAM-/CD133-	CK7+/NCAM+/CD133-
Notch pathway	x	x	↑↑↑
WNT pathway	↑↑↑	↑	↑↑↑

Figure 6 Proposed model for hepatic progenitor cell activation/differentiation. CD133, prominin 1; HPC, hepatic progenitor cell; K7, keratin 7; NCAM, neural cell adhesion molecule. (A) Schematic figure of HPC activation and differentiation. CD133 loss is a key feature of HPC differentiation. the Wnt pathway activation plays a key role for stem cell niche expansion. the presence of Notch signal drives the hpcs fate choice towards cholangiocytic lineage. (B) Different expression of hpcs markers and Wnt/Notch pathways in the liver diseases under study.

a result, the prominent HPC activation is not sufficient to restore cholangiocyte loss. In addition, the observation that 'stemness' genes ESRRB and NANOG were up regulated in PBC confirm a lack of terminal differentiation.

In haematopoietic, intestinal and neuronal stem cell niche, the modulation of Notch activity is fundamental in influencing the fate of progenitor cells.[45] The role of the Notch pathway in bile-duct development first became apparent in Alagille syndrome,[49] where mutations in the Jagged-1 gene (*JAG1*) were identified as the cause of Alagille syndrome causing bile-duct paucity. In general, Notch2 is responsible for the morphogenesis of forming bile-duct structures.[20 23] Notch 1 and 3 play an important role in biliary differentiation and maintenance in murine models.[31] In the present study lower *JAG1* encoding

mRNA in hepatocytic diseases (HCV and AH) was measured. Although protein expression of Jagged-1 did not correlate with the gene expression in AH (where it was still present on the HPCs), the lack of nuclear Notch staining in HCV (and increased nuclear staining in PBC) suggests a probable inhibition of this pathway in hepatocytic diseases. The increased values of *JAG1* and nuclear Notch1/NICD staining in PBC could be linked with fate choice towards cholangiocytes. This is in agreement with the observation that immature and mature cholangiocytes express members of the Notch pathway in vivo.[50] In rodent models Notch was found to play an important role in biliary differentiation of HPCs in a model of biliary ductopenia,[20 23] and after partial hepatectomy.[51 52] Our data suggest that Notch plays a similar role in biliary differentiation of human HPCs.

In most conditions the Notch signal requires physical contact between cells.[53 54] The observation that desmin positive myofibroblasts are mostly present surrounding HPCs during PBC indicates that these cells might be responsible for the (Notch) cell–cell communication between progenitor cells and mesenchymal cells regulating their bipotential cell fate which remains to be determined by functional assays.

Other pathways which were found to be of interest in this study included BMI1, a transcriptional receptor belonging to the polycomb group gene family,[55] which was present in all groups with a slight (non-significant) increase in the PBC group (data not shown). In the liver, BMI1 has been associated with ductopenia and an increased malignancy of HCC.[56 57] Due to the involvement of stem cell self-renewal of BMI1, this could indicate the increased self-renewal capacity of HPCs during liver disease.[58] In addition, from the hedgehog signalling pathway both Desert hedgehog as well as Sonic hedgehog were both expressed by HPCs (data not show). Recently Sonic hedgehog has been shown to be involved in epithelial-to-mesenchymal transition of ductular cells in non-alcoholic fatty liver disease.[59] If epithelial-to-mesenchymal transition does occur in HPCs during AH, HCV, and PBC remains to be proven.

Controlled manipulation of the HPC niche holds great promise for therapeutic intervention in currently untreatable liver diseases.[60–62] Although some of these treatments (such as γ-secretase inhibitors) mostly rely on Wnt or Notch inhibition in neoplastic diseases,[63] these treatments might be used to stimulate a patient's own progenitor cell compartment.

In conclusion, our gene expression analysis and immunohistochemical study on human liver diseases indicate that: (1) CD133 represents a surface marker for a restricted population of expanding HPCs associated with high AFP expression; (2) activation of the Wnt pathway plays a significant role in HPC expansion; and (3) the Notch pathway is involved in the fate choice of HPCs towards the cholangiocytic lineage. Functional assays should confirm these findings. These results hold great promise for development of future therapeutic strategies.

Acknowledgements We wish to thank Martine Gilis and Olivier Govaere for their technical assistance and Brigitte Arends for her thorough reading of the manuscript.

Funding This study was partially funded by the Funds for Scientific Research Flanders (FWO).

Competing interests None.

Ethics approval The use of the tissues in this research is allowed by Belgian law (19-12-2008 articles 2 and 20). This study was conducted with the approval of the Local Commission for Medical Ethics and Clinical Studies of the University of Leuven given on 7 November 2003.

Provenance and peer review Not commissioned; externally peer reviewed.

REFERENCES

1. **Alison MR,** Golding MH, Sarraf CE. Pluripotential liver stem cells: facultative stem cells located in the biliary tree. *Cell Prolif* 1996;**29**:373–402.
2. **Fausto N.** Liver regeneration and repair: hepatocytes, progenitor cells, and stem cells. *Hepatology* 2004;**39**:1477–87.
3. **Roskams TA,** Libbrecht L, Desmet VJ. Progenitor cells in diseased human liver. *Semin Liver Dis* 2003;**23**:385–96.
4. **Thorgeirsson SS.** Hepatic stem cells in liver regeneration. *FASEB J* 1996;**10**:1249–56.
5. **Alison M.** Liver stem cells: a two compartment system. *Curr Opin Cell Biol* 1998;**10**:710–5.
6. **Forbes S,** Vig P, Poulsom R, *et al*. Hepatic stem cells. *J Pathol* 2002;**197**:510–18.
7. **Zhang L,** Theise N, Chua M, *et al*. The stem cell niche of human livers: symmetry between development and regeneration. *Hepatology* 2008; **48**:1598–607.
8. **Roskams TA,** Theise ND, Balabaud C, *et al*. Nomenclature of the finer branches of the biliary tree: canals, ductules, and ductular reactions in human livers. *Hepatology* 2004;**39**:1739–45.
9. **Theise ND,** Saxena R, Portmann BC, *et al*. The canals of Hering and hepatic stem cells in humans. *Hepatology* 1999;**30**:1425–33.
10. **Clouston AD,** Powell EE, Walsh MJ, *et al*. Fibrosis correlates with a ductular reaction in hepatitis C: roles of impaired replication, progenitor cells and steatosis. *Hepatology* 2005;**41**:809–18.
11. **Desmet V,** Roskams T, Van EP. Ductular reaction in the liver. *Pathol Res Pract* 1995;**191**:513–24.
12. **Bird TG,** Lorenzini S, Forbes SJ. Activation of stem cells in hepatic diseases. *Cell Tissue Res* 2008;**331**:283–300.
13. **Paku S,** Nagy P, Kopper L, *et al*. 2-acetylaminofluorene dose-dependent differentiation of rat oval cells into hepatocytes: confocal and electron microscopic studies. *Hepatology* 2004;**39**:1353–61.
14. **Jones DL,** Wagers AJ. No place like home: anatomy and function of the stem cell niche. *Nat Rev Mol Cell Biol* 2008;**9**:11–21.
15. **Scadden DT.** The stem-cell niche as an entity of action. *Nature* 2006;**441**:1075–9.
16. **Barker N,** van de Wetering M, Clevers H. The intestinal stem cell. *Genes Dev* 2008;**22**:1856–64.
17. **Moore KA,** Lemischka IR. Stem cells and their niches. *Science* 2006;**311**:1880–5.
18. **Scoville DH,** Sato T, He XC, *et al*. Current view: intestinal stem cells and signaling. *Gastroenterology* 2008;**134**:849–64.
19. **Waters JM,** Richardson GD, Jahoda CA. Hair follicle stem cells. *Semin Cell Dev Biol* 2007;**18**:245–54.
20. **Geisler F,** Nagl F, Mazur PK, *et al*. Liver-specific inactivation of Notch2, but not Notch1, compromises intrahepatic bile duct development in mice. *Hepatology* 2008;**48**:607–16.
21. **Hay DC,** Fletcher J, Payne C, *et al*. Highly efficient differentiation of hESCs to functional hepatic endoderm requires ActivinA and Wnt3a signaling. *Proc Natl Acad Sci U S A* 2008;**105**:12301–6.
22. **Kodama Y,** Hijikata M, Kageyama R, *et al*. The role of notch signaling in the development of intrahepatic bile ducts. *Gastroenterology* 2004;**127**:1775–86.
23. **Lozier J,** McCright B, Gridley T. Notch signaling regulates bile duct morphogenesis in mice. *PLoS One* 2008;**3**:e1851.
24. **Micsenyi A,** Tan X, Sneddon T, *et al*. Beta-catenin is temporally regulated during normal liver development. *Gastroenterology* 2004;**126**:1134–46.
25. **Ober EA,** Verkade H, Field HA, *et al*. Mesodermal Wnt2b signalling positively regulates liver specification. *Nature* 2006;**442**:688–91.
26. **Tanimizu N,** Miyajima A. Notch signaling controls hepatoblast differentiation by altering the expression of liver-enriched transcription factors. *J Cell Sci* 2004;**117**:3165–74.
27. **Thompson MD,** Monga SP. WNT/beta-catenin signaling in liver health and disease. *Hepatology* 2007;**45**:1298–305.
28. **Apte U,** Thompson MD, Cui S, *et al*. Wnt/beta-catenin signaling mediates oval cell response in rodents. *Hepatology* 2008;**47**:288–95.
29. **Flynn DM,** Nijjar S, Hubscher SG, *et al*. The role of Notch receptor expression in bile duct development and disease. *J Pathol* 2004;**204**:55–64.
30. **Hu M,** Kurobe M, Jeong YJ, *et al*. Wnt/beta-catenin signaling in murine hepatic transit amplifying progenitor cells. *Gastroenterology* 2007;**133**:1579–91.
31. **Jensen CH,** Jauho EI, Santoni-Rugiu E, *et al*. Transit-amplifying ductular (oval) cells and their hepatocytic progeny are characterized by a novel and distinctive expression of delta-like protein/preadipocyte factor 1/fetal antigen 1. *Am J Pathol* 2004;**164**:1347–59.
32. **Caretti E,** Devarajan K, Coudry R, *et al*. Comparison of RNA amplification methods and chip platforms for microarray analysis of samples processed by laser capture microdissection. *J Cell Biochem* 2008;**103**:556–63.
33. **Thorgeirsson SS.** Hepatic stem cells. *Am J Pathol* 1993;**142**:1331–3.
34. **Roskams T.** Progenitor cell involvement in cirrhotic human liver diseases: from controversy to consensus. *J Hepatol* 2003;**39**:431–4.
35. **Roskams T.** Different types of liver progenitor cells and their niches. *J Hepatol* 2006;**45**:1–4.
36. **Yovchev MI,** Grozdanov PN, Joseph B, *et al*. Novel hepatic progenitor cell surface markers in the adult rat liver. *Hepatology* 2007;**45**:139–49.
37. **Song W,** Li H, Tao K, *et al*. Expression and clinical significance of the stem cell marker CD133 in hepatocellular carcinoma. *Int J Clin Pract* 2008;**62**:1212–18.

38. **Van Den Heuvel MC,** Slooff MJ, Visser L, *et al*. Expression of anti-OV6 antibody and anti-N-CAM antibody along the biliary line of normal and diseased human livers. *Hepatology* 2001;**33**:1387—93.
39. **Theise ND,** Badve S, Saxena R, *et al*. Derivation of hepatocytes from bone marrow cells in mice after radiation-induced myeloablation. *Hepatology* 2000;**31**:235—40.
40. **Kanazawa Y,** Verma IM. Little evidence of bone marrow-derived hepatocytes in the replacement of injured liver. *Proc Natl Acad Sci U S A* 2003;**100**:11850—3.
41. **Vig P,** Russo FP, Edwards RJ, *et al*. The sources of parenchymal regeneration after chronic hepatocellular liver injury in mice. *Hepatology* 2006;**43**:316—24.
42. **Kordes C,** Sawitza I, Muller-Marbach A, *et al*. CD133+ hepatic stellate cells are progenitor cells. *Biochem Biophys Res Commun* 2007;**352**:410—7.
43. **Naveiras O,** Daley GQ. Stem cells and their niche: a matter of fate. *Cell Mol Life Sci* 2006;**63**:760—6.
44. **Katoonizadeh A,** Nevens F, Verslype C, *et al*. Liver regeneration in acute severe liver impairment: a clinicopathological correlation study. *Liver Int* 2006;**26**:1225—33.
45. **Crosnier C,** Stamataki D, Lewis J. Organizing cell renewal in the intestine: stem cells, signals and combinatorial control. *Nat Rev Genet* 2006;**7**:349—59.
46. **Yang W,** Yan HX, Chen L, *et al*. Wnt/beta-catenin signaling contributes to activation of normal and tumorigenic liver progenitor cells. *Cancer Res* 2008;**68**:4287—95.
47. **Zhang Y,** Li XM, Zhang FK, *et al*. Activation of canonical Wnt signaling pathway promotes proliferation and self-renewal of rat hepatic oval cell line WB-F344 in vitro. *World J Gastroenterol* 2008;**14**:6673—80.
48. **Zhou H,** Rogler LE, Teperman L, *et al*. Identification of hepatocytic and bile ductular cell lineages and candidate stem cells in bipolar ductular reactions in cirrhotic human liver. *Heptology* 2007;**45**:716—24.
49. **Piccoli DA,** Spinner NB. Alagille syndrome and the Jagged1 gene. *Semin Liver Dis* 2001;**21**:525—34.
50. **Nijjar SS,** Crosby HA, Wallace L, *et al*. Notch receptor expression in adult human liver: a possible role in bile duct formation and hepatic neovascularization. *Hepatology* 2001;**34**:1184—92.
51. **Kohler C,** Bell AW, Bowen WC, *et al*. Expression of Notch-1 and its ligand Jagged-1 in rat liver during liver regeneration. *Hepatology* 2004;**39**:1056—65.
52. **Xu HY,** Li BJ, Wang RF, *et al*. Alterations of Notch/Jagged mRNA and protein expression after partial hepatectomy in rats. *Scand J Gastroenterol* 2008;**43**:1522—8.
53. **Fortini ME.** Notch signaling: the core pathway and its posttranslational regulation. *Dev Cell* 2009;**16**:633—47.
54. **Kopan R,** Ilagan MX. The canonical Notch signaling pathway: unfolding the activation mechanism. *Cell* 2009;**137**:216—33.
55. **van der Lugt NM,** Domen J, Linders K, *et al*. Posterior transformation, neurological abnormalities, and severe hematopoietic defects in mice with a targeted deletion of the bmi-1 proto-oncogene. *Genes Dev* 1994;**8**:757—69.
56. **Sasaki M,** Ikeda H, Sato Y, *et al*. Decreased expression of Bmi1 is closely associated with cellular senescence in small bile ducts in primary biliary cirrhosis. *Am J Pathol* 2006;**169**:831—45.
57. **Wang H,** Pan K, Zhang HK, *et al*. Increased polycomb-group oncogene Bmi-1 expression correlates with poor prognosis in hepatocellular carcinoma. *J Cancer Res Clin Oncol* 2008;**134**:535—41.
58. **Park IK,** Qian D, Kiel M, *et al*. Bmi-1 is required for maintenance of adult self-renewing haematopoietic stem cells. *Nature* 2003;**423**:302—5.
59. **Syn WK,** Omenetti A, Abdelmalek M, *et al*. Hedgehog-Mediated Epithelial-to-Mesenchymal Transition and Fibrogenic Repair in Non-Alcoholic Fatty Liver Disease. *Gastroenterology* 2009;**2**. doi:10.1053/j.gastro.2009.06.051.
60. **Alison MR,** Choong C, Lim S. Application of liver stem cells for cell therapy. *Semin Cell Dev Biol* 2007;**18**:819—26.
61. **Prockop DJ,** Olson SD. Clinical trials with adult stem/progenitor cells for tissue repair: let's not overlook some essential precautions. *Blood* 2007;**109**:3147—51.
62. **Shafritz DA,** Oertel M, Menthena A, *et al*. Liver stem cells and prospects for liver reconstitution by transplanted cells. *Hepatology* 2006;**43**:S89—98.
63. **van Es JH,** Clevers H. Notch and Wnt inhibitors as potential new drugs for intestinal neoplastic disease. *Trends Mol Med* 2005;**11**:496—502.